Ultra-Fast Fluorescence Anisotropy Decay of *N*-Acetyl-L-Tryptophanamide Reports on the Apparent Microscopic Viscosity of Aqueous Solutions of Guanidine Hydrochloride

Antonie J.W.G. Visser, Nina V. Visser, Arie van Hoek, and Herbert van Amerongen

Abstract The very fast fluorescence anisotropy decay of *N*-acetyl-L-tryptophanamide (NATA) in aqueous solutions has been measured with sub-picosecond laser excitation and detection with time-correlated single photon counting. By using global analysis of both parallel and perpendicular polarized fluorescence intensity decays involving deconvolution, the rotational correlation times of NATA in the tens of picosecond range are accurately recovered. Since rotational correlation times are directly proportional to viscosity, we have used these correlation times to derive the (relative) microscopic viscosity of increasing concentrations of guanidine hydrochloride (GuHCl) in buffered water. GuHCl is a well-known chaotropic agent of protein denaturation. We give a step-by-step description how to obtain the final results. Subsequently, we compare the obtained microscopic viscosities with macroscopic viscosity data reported half a century ago using capillary viscosimeters. From the results it is clear that GuHCl, present in molar concentration, associates with NATA making the apparent molecular volume larger.

Keywords Fluorescence anisotropy • Fluorescence lifetime • Fluorescence polarization • Global analysis • Microscopic and macroscopic viscosity • Protein denaturant • Time-correlated single photon counting • Tryptophan fluorescence

A.J.W.G. Visser (✉)
Laboratory of Biochemistry, Microspectroscopy Centre, Wageningen University, P.O. Box 8128, 6700 ET Wageningen, The Netherlands
e-mail: antoniejvisser@gmail.com

N.V. Visser, A. van Hoek, and H. van Amerongen
Laboratory of Biophysics, Microspectroscopy Centre, Wageningen University, P.O. Box 8128, 6700 ET Wageningen, The Netherlands

D.M. Jameson (ed.), *Perspectives on Fluorescence: A Tribute to Gregorio Weber*,
Springer Ser Fluoresc (2016) 17: 81–94, DOI 10.1007/4243_2016_11,

Contents

1 Introduction

Gregorio Weber played a pioneering role in developing protein fluorescence in all its modern facets. In 1957 Gregorio Weber and his co-worker John Teale published the first corrected emission and excitation spectra of the aromatic amino acids: phenylalanine, tyrosine, and tryptophan [1]. A few years later Weber published fluorescence polarization as function of excitation wavelength (polarization spectrum) of tyrosine, tryptophan, and related compounds (phenol and indole) in cryogenic solutions [2] and of the same amino acid residues in proteins at both ambient and low temperature [3]. From measurements in more concentrated solutions of the individual compounds and mixtures a distinct depolarization was observed, which could be ascribed to electronic energy transfer between the same molecules (homotransfer) or between different molecules (heterotransfer) [2]. Similar depolarization processes in proteins indicate, depending on the particular protein, the occurrence of homotransfer between tyrosine or tryptophan residues or heterotransfer from tyrosine to tryptophan residues [3]. Many researchers now refer to Förster Resonance Energy Transfer or FRET for this process instead of electronic energy transfer. In 1977 Bernard Valeur and Gregorio Weber published polarization spectra of indole and tryptophan in cryogenic solutions to spectrally resolve the ^1L_a and ^1L_b electronic transitions, which are close in energy [4]. The ^1L_a transition is in most cases the emitting state and it can be selectively excited without much interference of the ^1L_b transition when excitation wavelengths are >300 nm. Already in the final chapter of Gregorio Weber's PhD thesis (published in 1947) it was shown that fluorescence polarization can be used to determine the internal viscosity (or microscopic viscosity) of gels. When the molecular dimension of the

fluorescent molecule (the solute) is large as compared to the one of solvent molecules, the microscopic viscosity, which determines the resistance (or friction) to rotational diffusion, is the same as that determined from the resistance of the solvent to flow (or macroscopic viscosity). When the molecular dimensions of solute and solvent are similar, microscopic and macroscopic viscosities may differ markedly. The actual (first) publication on viscosity measurements with fluorescence polarization in gel systems such as micelles appeared much later [5].

In this chapter we report on ultra-fast fluorescence anisotropy decay of the well-known tryptophan (Trp) analogue *N*-acetyl-L-tryptophanamide (NATA) in aqueous solutions of increasing concentrations of the protein denaturant guanidine hydrochloride (GuHCl). Previously, we have used GuHCl to investigate denaturant-induced (un)folding of apoflavodoxin from *Azotobacter vinelandii* with polarized time-resolved fluorescence methods [6, 7]. Using picosecond-resolved fluorescence anisotropy of wild-type apoflavodoxin containing three tryptophan residues and of mutant proteins lacking one or two Trps, it has been demonstrated that photo-excited tryptophan residues of apoflavodoxin exchange energy through a FRET mechanism [7]. Energy transfer from Trp167 to Trp128, residues that are 6.8 Å apart, leads to a rapid decay of the experimental anisotropy signal with a unidirectional 50-ps transfer correlation time [7]. FRET between the other Trp-Trp couples turned out to be much slower or even absent. The short rotational correlation time of NATA in aqueous solutions, obtainable from analysis of time-resolved fluorescence anisotropy, will be a challenging test case to recover ultra-fast depolarization processes of the type described in [7]. The protocol how to obtain these correlation times, which are even shorter than the FWHM of the impulse response function, is the subject of this chapter. In addition, the results will show that aqueous GuHCl solutions cannot be considered as a homogeneous solvent, since the denaturant exhibits molecular interaction with NATA that lasts much longer than the fluorescence lifetime.

2 Experimental Section

2.1 Materials and Solutions

Scintillation grade *p*-terphenyl and *N*-acetyl-L-tryptophanamide were purchased from BDH and Sigma, respectively. Spectroscopically pure cyclohexane and spectrophotometric grade carbon tetrachloride (CCl_4) were purchased from Merck and Janssen Chimica, respectively. 1 μM of *p*-terphenyl in cyclohexane/CCl_4 (50/50 v/v) has been used as a reference compound [8]. Aqueous solutions of different concentrations of guanidine chloride (GuHCl) in 100 nM potassium pyrophosphate buffer (pH 6.0) were prepared as previously described [7]. The final concentration of NATA amounted to 4.4 μM. The temperature of all experiments was 25°C.

2.2 Measurement Setup

Time-resolved fluorescence measurements were performed using mode-locked continuous wave lasers for excitation and the time-correlated single photon counting (TCSPC) technique for detection as described elsewhere [9]. We will summarize the main elements of the setup. For elaborate functional details and manufacturers of the different parts, we refer to the previous publication [9]. The pump laser was a CW diode-pumped, frequency-doubled Nd:YVO_4 laser and the mode-locked laser was a titanium: sapphire laser (in fs mode) tuned to 900 nm. At the output of the titanium: sapphire laser a pulse picker was placed, decreasing the repetition rate of excitation pulses to 3.8×10^6 pulses per second (3.8 MHz). The output of the pulse picker was directed towards a frequency tripler. For excitation a maximum pulse energy of sub-pJ was used, the wavelength was 300 nm and the pulse duration about 0.2 ps. An excitation wavelength of 300 nm was chosen because then the highest initial anisotropy was obtained by selective excitation in the ^1L_a transition of the indole ring [4]. The samples were in 1.5 mL and 10-mm light path fused silica cuvettes in a temperature controlled sample holder, which was placed in a housing also containing the main detection optics. Extreme care was taken to avoid artifacts from depolarization effects. At the front of the sample housing a Glan-laser polarizer was mounted, optimizing the already vertical polarization of the input light beam. The fluorescence was collected at an angle of 90° with respect to the direction of the exciting light beam. Both the sample and the photomultiplier detector were placed a single fast lens (uncoated fused silica, F/3.0), a Schott UV-DIL 348.8 nm ($\Delta\lambda = 5.4$ nm) interference filter, a rotatable sheet type polarizer (Polaroid type HNP'B suitable for ultraviolet radiation), and a second single fast lens (uncoated fused silica, F/3.0) focusing the fluorescence on the photomultiplier cathode. The polarizer sheet was in a dc motor driven ball-bearing holder with mechanical stops, allowing computer-controlled rotation (0.2 s) to parallel and perpendicular polarized detection of emission. The polarizers were carefully aligned and the performance of the setup finally checked by measuring suitable reference samples [10]. Detection electronics were TCSPC modules detailed in [9]. A microchannel plate photomultiplier was used for the detection of the fluorescence photons. The single photon responses of this photomultiplier were processed as previously described and finally collected in 4096 channels of a multichannel analyzer. The channel time spacing was 5.0 ps. By reducing the energy of the excitation pulses with neutral density filters, the rate of fluorescence photons was decreased to less than 30,000 per second (≈1% of 3.8 MHz), to prevent pile-up distortion. For the deconvolution procedure, the dynamic instrumental response function was determined using a freshly made solution of *p*-terphenyl in a mixture of 50/50 (v/v) cyclohexane and CCl_4 [8]. One complete measurement consisted of the recording of three cycles of the parallel (10 s) and perpendicularly (10 s) polarized fluorescence of the reference compound, ten cycles of parallel (10 s) and perpendicularly (10 s) polarized fluorescence of the sample, and two cycles of polarized background emission of the buffer (with increasing amounts of GuHCl) measured under the same conditions as the sample and again the reference compound.

2.3 Data Analysis

Time-resolved polarized fluorescence data analysis was essentially as described by Borst and co-workers [9]. Global fitting of parallel and perpendicular polarized fluorescence intensity decays was performed using the "TRFA Data Processing Package" of the Scientific Software Technologies Center (www.sstcenter.com; Belarusian State University, Minsk, Belarus) [11]. For the deconvolution procedure, the dynamic instrumental response function was determined using a freshly made solution of *p*-terphenyl in cyclohexane/CCl_4 (50/50 v/v). Fluorescence lifetime analysis of NATA required a minimum model of a one-component model for good fitting. However, we will compare also a two-component model. After optimization of amplitudes and lifetimes of the total fluorescence, the time-dependent fluorescence anisotropy $r(t)$ is calculated from the parallel and perpendicular intensity components in which the initial anisotropy at zero time, $r(0)$, and the rotational correlation time, ϕ, are the fitting parameters. Global analysis was performed by simultaneous fitting of parallel and perpendicular polarized fluorescence intensity decays and linking the common correlation time ϕ and initial anisotropy $r(0)$. In addition, a rigorous error analysis at the 67% confidence level was applied to the optimized rotational correlation time.

3 Results

3.1 Searching for the Optimum Fluorescence Lifetime of the Reference Compound

In Ref. [12] a method is described to fit the fluorescence lifetime of the reference compound *p*-terphenyl in ethanol together with the fluorescence of NATA in water in the fluorescence decay analysis. This resulted in excellent fits giving a lifetime value of 1.07 ns for *p*-terphenyl in ethanol, which is insensitive to temperature between 4 and 30°C. In contrast, the fluorescence lifetime of NATA in water is sensitive to temperature giving values of 3.98 ns at 4°C, 3.01 ns at 20°C, and 2.48 ns at 30°C. For the fluorescence decay of *p*-terphenyl in cyclohexane, which is dynamically quenched by CCl_4, a similar procedure of using fluorescence lifetimes of quenched and unquenched *p*-terphenyl in cyclohexane as fitting parameters worked well leading to a fluorescence lifetime of 0.94 ns for *p*-terphenyl in cyclohexane and of 12 ps for *p*-terphenyl in cyclohexane/CCl_4 (50/50 v/v) at 20°C [8]. In this work we used a similar procedure by performing a single-component fluorescence decay analysis of NATA in water (pH 6.0) with *p*-terphenyl in cyclohexane/CCl_4 (50/50 v/v) as a reference compound at 25°C. When we systematically varied the fluorescence lifetime of the reference compound (τ_{ref}), performed the decay analysis, and listed the value of the fitting criterion χ^2, a minimum χ^2 is reached for $\tau_{ref} = 14$ ps (results not shown). It did not matter whether we took the fluorescence lifetime of NATA (2.72 ns) as fixed or free parameter in the analysis.

3.2 Total Fluorescence Decay Analysis of NATA in Aqueous Buffer

The fluorescence decay analysis of NATA in aqueous buffer is presented in Fig. 1. Three curves are presented in the upper panel as detailed in the legend of Fig. 1. At first sight a single lifetime component of 2.72 ns appears to be sufficient to describe the fluorescence decay of NATA, since there is no difference between both black

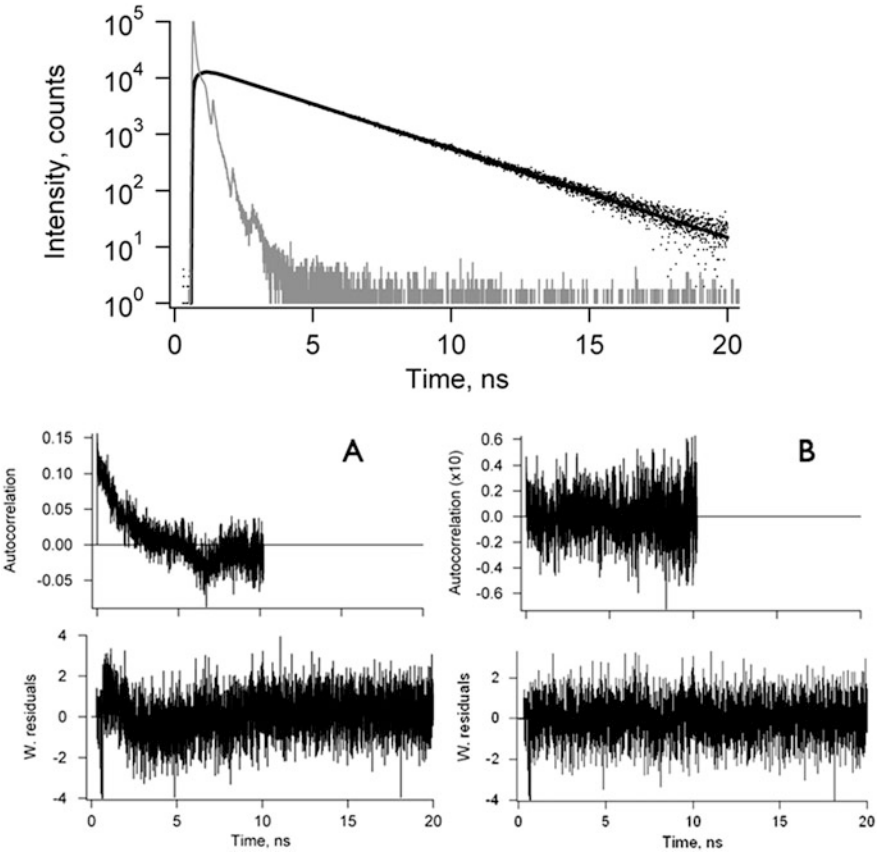

Fig. 1 *Top panel*. Fluorescence decay analysis of NATA in aqueous buffer. The figure shows the experimental fluorescence decay (*black dots*) and the fitted curve (*black solid line*) on a semi-logarithmic scale. In *grey* is the instrumental response function taken from a *p*-terphenyl cyclohexane/CCl_4 (50/50 v/v) solution. Fitting was accomplished over the complete rise and decay curve. The recovered fluorescence lifetime was 2.72 ns and the reduced χ^2 (i.e., fitting criterion) amounted to 1.17. *Lower panel*. Comparison between fits of one-exponential component (**a**) and of two-exponential components (**b**) applied to the same data. The first point in the autocorrelation function should always start with one, but it is suppressed for clarity. For the two-exponential fit the recovered fluorescence lifetimes were $\tau_1 = 1.3$ ns ($\alpha_1 = 0.07$) and $\tau_2 = 2.77$ ns ($\alpha_2 = 0.93$) and the reduced χ^2 amounted to 1.04. Note that in **b** the autocorrelation function is multiplied by 10

curves (dots and line) and the reduced χ^2 is equal to 1.17, which is sufficiently low. However, when other fitting criteria are presented, such as the presentation of weighted residuals and the autocorrelation of the weighted residuals (Fig. 1), the conclusion of a single fluorescence lifetime is not a firm one. The autocorrelation function of the residuals is a very good indicator of the goodness of a fit. This function clearly indicates that NATA fluorescence decay is not for 100% single exponential (Fig. 1, panel a), but a second, shorter component (~1.3 ns) of small amplitude (~7%) is needed to make both residuals and autocorrelation functions randomly fluctuate around zero (Fig. 1, panel b). We will address this apparent non-exponential behavior of the fluorescence decay of NATA in the discussion section.

3.3 Fluorescence Anisotropy Decay Analysis of NATA in Aqueous Buffer

The rotational correlation time of NATA in aqueous buffer will be extremely fast in the range of tens of picoseconds. It is therefore a large challenge to accurately determine these rotational correlation times from analysis of the fluorescence anisotropy decay. The complexity of the analysis is illustrated in four panels of Fig. 2. In Fig. 2a the normalized time traces of reference response curve, total fluorescence, and the experimental anisotropy recovered after deconvolution are shown. The reference response curve has a full width at half the maximum intensity (FWHM) of 80 ps, which is the same as the FWHM of the instrumental response function (IRF, results not shown) measured with TCSPC. The pure anisotropy after deconvolution shows a decay within the reference response curve. In addition, the fluorescence of NATA still has to be built up because of the finite width of the IRF.

Despite the ultra-short rotational correlation time of NATA in water, global analysis of the individual polarized fluorescence intensity components is advantageous as illustrated in Fig. 2b. Parallel and perpendicular polarized fluorescence curves are fitted very well over the whole rise and decay curves of NATA fluorescence. At this stage it is important to note that we used the best fitted total fluorescence decay profiles, since this will lead to the lowest total reduced χ^2. In this case the two-exponential fit of the total fluorescence decay is merely used as a mathematical function to optimally emulate the total fluorescence decay of NATA.

Rather than presenting the whole analyzed anisotropy curve between 0 and 20 ns, it is much more illustrative to present the most relevant part of the curve (see line markers at two time points in Fig. 2c). The experimental anisotropy points at the left side of the shortest time point become unstable, as the fluorescence intensity approaches zero. However, the fitted anisotropy points show a much clearer behavior (Fig. 2d), which makes the choice of the first point of presentation much easier. It corresponds to the time point where the maximum is reached. In Fig. 2c the left marker is placed at time $t = 0.625$ ns. The right marker at longer time

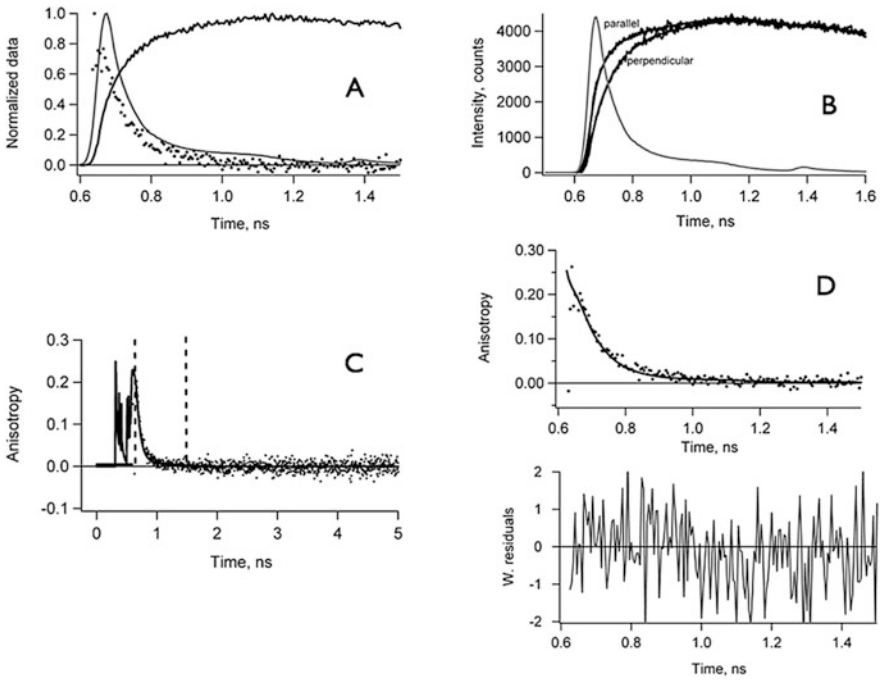

Fig. 2 Fluorescence anisotropy decay analysis of NATA in aqueous buffer. (**a**) Normalized curves on an expanded time scale to illustrate the time limits. Shown are the total fluorescence (*solid black line*), the anisotropy decay *after deconvolution* (*black points*), and the reference response curve (*grey*; 80 ps FWHM). (**b**) Global analysis of parallel and perpendicular polarized fluorescence. The experimental (noisy traces) and calculated curves (*solid lines*) are presented in *black* and the reference response curve is shown in *grey*. Analysis took place over the whole decay curves, but only the initial part is shown. Note that both polarized curves become indistinguishable after 1.2 ns. The reduced χ^2-values are for the parallel component 1.145 and for the perpendicular component 1.077. (**c**) Snapshot of the first 5 ns (out of 20 ns) of the observed (*dots*) and fitted (*line*) anisotropies and the borders within to present analysis details in panel **d**. (**d**) Deconvoluted fluorescence anisotropy decay of NATA in aqueous buffer. In the top panel the experimental (*points*) and the fitted data (*solid line*) are shown. In the lower panel the weighted residuals between experimental and fitted curves are presented. The recovered rotational correlation time $\phi = 43$ ps between 38 ps (lower bound confidence limit) and 48 ps (upper bound confidence limit). The initial anisotropy $r(0) = 0.261$

is placed rather arbitrarily, namely, where the anisotropy is completely decayed to zero. It is placed at $t = 1.5$ ns. In Fig. 2d a snapshot of anisotropy decay analysis corresponding to the two time markers is presented. The fit of experimental data points (175 channels) with an exponential function with single rotational correlation time $\phi = 43$ ps is nearly perfect as judged from the randomly distributed weighted residuals. The initial anisotropy $r(0) = 0.261$.

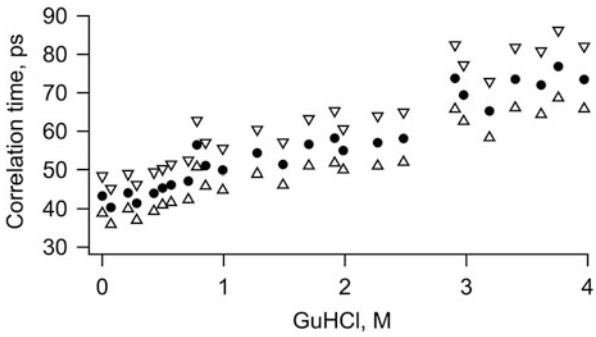

Fig. 3 Rotational correlation times (in picoseconds) of NATA in aqueous buffer versus the molar concentration of guanidine hydrochloride (GuHCl). Shown are the recovered correlation times (*closed circles*) and the upper (*open inverted triangle*) and lower (*open triangle*) confidence limits at the 67% level

3.4 Fluorescence Anisotropy Decay Analysis of NATA in Aqueous Buffer Containing GuHCl

The rotational correlation times of NATA in aqueous buffer containing increasing GuHCl concentrations are obtained after a similar analysis procedure described in the previous section. A bi-exponential fluorescence decay is assumed. The long fluorescence lifetime was pretty constant, namely 2.71 ± 0.06 ns, which is the same value as obtained for a one-exponential decay analysis. The other fluorescence lifetime component, which is present in small percentage, did not have a fixed value. The obtained overall χ^2 value amounted to 1.13 ± 0.03. Rotational correlation times are presented in Fig. 3. Upper and lower confidence limits at the 67% level are also presented in the same graph. It can be clearly seen that in most cases the upper confidence limit is larger than the lower one, which is due to the rigorous error analysis not giving Gaussian standard errors. The initial anisotropies are averaged yielding $r(0) = 0.251 \pm 0.019$. The correlation times become longer at higher GuHCl concentrations.

3.5 Relative Increase of Viscosity at Increasing GuHCl Concentration

The well-known Stokes-Einstein equation for spherical molecules gives the rotational diffusion coefficient D_r according to:

$$D_r = \frac{k_B T}{6\eta V_h} = \frac{k_B T}{8\pi\eta r_h^3} \tag{1}$$

where k_B is the Boltzmann constant, T is the absolute temperature, η is the viscosity of the medium, V_h is the hydrodynamic volume, and r_h is the hydrodynamic radius of the sphere. The rotational correlation time ϕ is equal to:

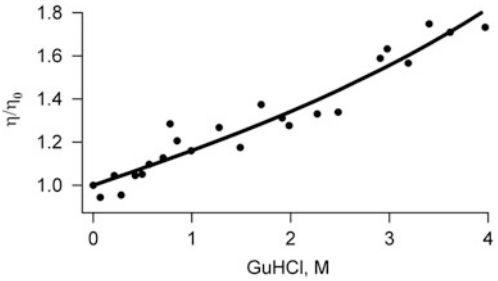

Fig. 4 Relative viscosity values (η/η_0) of NATA in aqueous buffer versus the molar concentration of guanidine hydrochloride (GuHCl). The experimental data are obtained by dividing the rotational correlation times of NATA by the one at [GuHCl] = 0 M, which corresponds to η_0. The solid line is a polynomial fit to the data points: $\eta/\eta_0 = 1 + 0.1571*x + 0.019*x^2 + 0.0025*x^3$, where x is [GuHCl]. Nonlinear least-squares curve fitting was accomplished with the Microsoft Excel Solver. In the fitting procedure the data points were weighted by 1/(standard error)^2

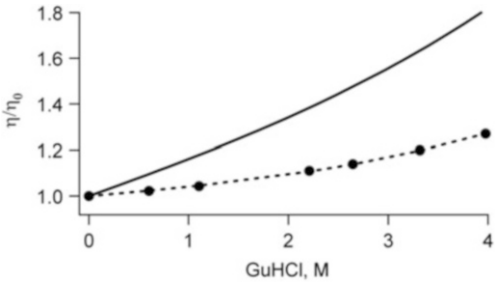

Fig. 5 Comparison of relative viscosities of aqueous solutions of guanidine hydrochloride obtained by us (*solid line*, see Fig. 4) and by Kawahara and Tanford [13] (*closed circles*). The experimental data of Kawahara and Tanford were fitted to a polynomial function (*dashed curve*) to the data points between 1 and 6 M GuHCl: $\eta/\eta_0 = 1 + 0.0385*x + 0.0009*x^2 + 0.0016*x^3$, where x is [GuHCl]. Fitting was accomplished as described in the legend of Fig. 4 with equal weighting factors

$$\phi = \frac{1}{6D_r} = \frac{\eta V_h}{k_B T} \tag{2}$$

The hydrodynamic volume of NATA is not necessarily that of a sphere, but is, in first approximation, assumed to be the same in all experiments. Therefore the rotational correlation time would be directly proportional to the viscosity η.

When all rotational correlations are divided by the one obtained in the absence of GuHCl, the relative viscosities are obtained and plotted in Fig. 4. The TRFA Data Processing Package does not only provide confidence limits of the parameters after a rigorous error analysis, but also standard errors. The standard errors can be used as weighting factors in a nonlinear fitting procedure to fit a polynomial function through the data points (solid line in Fig. 4; see corresponding legend).

Macroscopic viscosities of aqueous solutions of GuHCl at 25°C were determined using capillary viscosimeters about half a century ago [13]. These values are plotted together in Fig. 5 with the microscopic viscosities, as obtained in Fig. 4. We

will discuss the relative large differences between relative macroscopic and microscopic viscosities in the discussion section.

4 Discussion

4.1 Is NATA a Single Fluorescence Lifetime Standard?

Szabo and Rayner observed that the fluorescence decay of tryptophan in aqueous solution (at 20°C and pH 7) exhibits two lifetime components of 3.1 and 0.5 ns with fluorescence maxima at 350 and 335 nm, respectively [14]. The authors assigned the different lifetimes to different rotamers of the alanyl side chain of tryptophan. Three predominant rotameric structures exist for tryptophan. The heterogeneity of the tryptophan environment was corroborated by hybrid quantum mechanical and molecular mechanical simulations of both wavelengths and lifetimes for rotamers of tryptophan in different cyclic hexapeptides [15]. The latter simulations indeed reveal that rotamers having blue-shifted emission possess shorter average fluorescence lifetimes than those having red-shifted emission. The different fluorescence lifetimes of rotameric states of tryptophan reflect differences in rates of photo-induced electron transfer from indole to the alanyl part.

NATA in water at 20°C is considered to have a mono-exponential fluorescence decay, which fluorescence lifetime amounts to 3.1 ± 0.1 ns [10]. However, if we look at the autocorrelation function of the weighted residuals in Fig. 1, there is not a perfect match with one lifetime, while the match is nearly perfect with two lifetime components of 1.3 ns (7%) and 2.77 ns (93%). Similar observations are reported by Rolinski and co-workers, who found that the fluorescence decay of NATA could not be fitted to one- or two-exponential functions because of unacceptably high χ^2 values [16]. Instead, the latter authors find a reasonable fit from a maximum entropy method using gamma function distributions peaking at $\tau_F = 3.0$ ns with ~0.5-ns FWHM at 23°C. The distributions are attributed to a single rotamer. For NATA the distribution is broad with τ_F strongly dependent on temperature. Each distribution also shows a distribution of much smaller amplitude with a peak between 1 and 1.5 ns, which was tentatively interpreted as a much less populated rotamer involved in more efficient photo-induced electron transfer from indole to the amide group [16]. This smaller distribution may have the same origin as the second lifetime of 1.3 ns found in our work.

Recent near microsecond molecular dynamics simulations of NATA in water indicate that there is a mixture of rotamers that interchange on a time scale similar to the excited state lifetime leading to a single exponential decay [17]. In these simulations two rotameric species are assumed, one in which the energy gap between the charge transfer state and emitting ^1L_a state is far apart (F state) for effective quenching and one in which the energy gap is close (C state) resulting in strong fluorescence quenching by electron transfer to the amide.

4.2 Microscopic and Macroscopic Viscosities

The relative microscopic and macroscopic viscosities of aqueous solutions of guanidine hydrochloride, plotted in Fig. 5, become increasingly different at higher concentration of GuHCl. At 4 M GuHCl the relative microscopic viscosity is 1.81, which is significantly larger than the relative macroscopic viscosity of 1.27. The ratio of these numbers is 1.42. A very likely explanation is that the apparent hydrodynamic volume V_h in Eq. (1) becomes larger. This can be caused by association of GuHCl molecules to NATA, for example, by hydrogen bonding facilitated by water molecules. When this hydrogen-bonding interaction persists much longer than the fluorescence lifetime of NATA, then the rotation of NATA will be slower, since GuHCl molecules are dragged along, thus making the effective size of NATA larger. When it is assumed that in first approximation the relative increase in V_h is proportional to the relative increase of molecular weights, then a simple calculation shows that $(MW_{NATA}+MW_{GuHCl})/MW_{NATA} = (245.28 + 95.53)/245.28 = 1.39$, which is very close to the above-mentioned ratio of 1.42 suggesting that a 1:1 complex is formed. The equilibrium dissociation constant of this weak complex would be in the order of a few molar of GuHCl. We can conclude that aqueous solutions of the strong chaotropic agent GuHCl cannot be considered as a homogeneous solvent such as glycerol/water mixtures.

How can we prove that GuHCl associates with NATA? Microsecond molecular dynamics simulations as described above for NATA in water [17] may provide the answer. In this case analysis of molecular dynamics trajectories of NATA (in the excited singlet state) in a water box with an excess of GuHCl molecules might indicate the presence of these long lasting hydrogen-bonding networks.

5 Conclusions

Comparison of macroscopic and microscopic viscosities shows an antagonistic effect. In contrast to most other observations, the microscopic viscosity, measured via time-resolved fluorescence depolarization of NATA, is larger than the macroscopic one, measured with capillary viscosimeters without NATA. This apparent discrepancy must be ascribed to formation of a weak complex between NATA and GuHCl making the apparent hydrodynamic volume larger. Finally, one may wonder whether steady-state fluorescence anisotropy, $\langle r \rangle$, will yield the same conclusive results. For calculation of $\langle r \rangle$ the following relationship is used:

$$\langle r \rangle = r(0)\frac{\phi}{\tau_F + \phi} \tag{3}$$

with all parameters already defined. With $r(0) = 0.251$ and $\tau_F = 2.71$ ns we find $\langle r \rangle = 0.004$ for $\phi = 0.043$ ns (0 M GuHCl) and $\langle r \rangle = 0.007$ for $\phi = 0.073$ ns (4 M

GuHCl). In other words, one should measure the steady-state fluorescence anisotropy with a precision better than 0.001 to obtain the same results. Therefore, the time-resolved fluorescence anisotropy experiment offers a much larger dynamic range than its steady-state counterpart.

Acknowledgments NVV was supported by The Netherlands Organization for Scientific Research.

References

1. Teale FWJ, Weber G (1957) Ultraviolet fluorescence of the aromatic amino acids. Biochem J 65:476–482
2. Weber G (1960) Fluorescence polarization spectrum and electronic energy transfer in tyrosine, tryptophan and related compounds. Biochem J 75:335–345
3. Weber G (1960) Fluorescence polarization spectrum and electronic energy transfer in proteins. Biochem J 75:345–352
4. Valeur B, Weber G (1977) Resolution of the fluorescence excitation spectrum of indole into the ^1L_a and ^1L_b excitation bands. Photochem Photobiol 25:441–444
5. Shinitzky M, Dianoux AC, Gitler C, Weber G (1971) Microviscosity and order in the hydrocarbon region of micelles and membranes determined with fluorescent probes. I. Synthetic micelles. Biochemistry 10:2106–2113
6. Laptenok SP, Visser NV, Engel R, Westphal AH, van Hoek A, van Mierlo CP, van Stokkum IH, van Amerongen H, Visser AJ (2011) A general approach for detecting folding intermediates from steady-state and time-resolved fluorescence of single-tryptophan-containing proteins. Biochemistry 50:3441–3450
7. Visser NV, Westphal AH, van Hoek A, van Mierlo CP, Visser AJ, van Amerongen H (2008) Tryptophan-tryptophan energy migration as a tool to follow apoflavodoxin folding. Biophys J 95:2462–2469
8. Visser NV, Visser AJ, Konc T, Kroh P, van Hoek A (1994) New reference compound with single, ultrashort lifetime for time-resolved tryptophan fluorescence experiments. Proc SPIE 2137:618–626
9. Borst JW, Hink MA, van Hoek A, Visser AJ (2005) Effects of refractive index and viscosity on fluorescence and anisotropy decays of enhanced cyan and yellow fluorescent proteins. J Fluoresc 15:153–160
10. Boens N, Qin W, Basaric N, Hofkens J, Ameloot M, Pouget J, Lefevre JP, Valeur B, Gratton E, vandeVen M, Silva ND Jr, Engelborghs Y, Willaert K, Sillen A, Rumbles G, Phillips D, Visser AJ, van Hoek A, Lakowicz JR, Malak H, Gryczynski I, Szabo AG, Krajcarski DT, Tamai N, Miura A (2007) Fluorescence lifetime standards for time and frequency domain fluorescence spectroscopy. Anal Chem 79:2137–2149
11. Digris AV, Novikov EG, Skakun VV, Apanasovich VV (2014) Global analysis of time-resolved fluorescence data. Methods Mol Biol 1076:257–277
12. Vos K, van Hoek A, Visser AJ (1987) Application of a reference convolution method to tryptophan fluorescence in proteins. A refined description of rotational dynamics. Eur J Biochem 165:55–63
13. Kawahara K, Tanford C (1966) Viscosity and density of aqueous solutions of urea and guanidine hydrochloride. J Biol Chem 241:3228–3232
14. Szabo AG, Rayner DM (1980) Fluorescence decay of tryptophan conformers in aqueous solution. J Am Chem Soc 102:554–563

15. Pan CP, Muino PL, Barkley MD, Callis PR (2011) Correlation of tryptophan fluorescence spectral shifts and lifetimes arising directly from heterogeneous environment. J Phys Chem B 115:3245–3253
16. Rolinski OJ, Scobie K, Birch DJS (2009) Protein fluorescence decay: a gamma function description of thermally induced interconversion of amino acid rotamers. Phys Rev E 79:050901
17. Callis PR, Tusell JR (2014) MD+QM correlations with tryptophan fluorescence spectral shifts and lifetimes. Methods Mol Biol 1076:171–214